Route Preview in Energy Management of Plug-in Hybrid Vehicles

Chen Zhang and Ardalan Vahidi

***Abstract*—This brief evaluates the use of terrain, vehicle speed, and trip distance preview to increase the fuel economy of plug-in hybrid vehicles. Access to future information is classified into full, partial, or no future information and for each case an energy management strategy with the potential for a real-time implementation is proposed. With full knowledge of future driving conditions, dynamic programming (DP) provides a best-achievable benchmark. A partial preview level has access to future trip terrain and requires velocity estimation. Equivalent consumption minimization strategy (ECMS) is deployed as an instantaneous *real-time* minimization strategy with parameters adjusted by estimated future driving conditions and obtained either from DP or from a backward solution of ECMS. To reduce the requirement for future velocity and detailed terrain information, another partial preview level only assumes known trip distance to the next charging station and elevation changes (if available). In this level, the parameter of the *real-time* ECMS is estimated based on the remaining trip distance, the battery's state-of-charge, and elevation changes if included. The results are evaluated against cases with no preview. Results from a number of simulation case studies indicate that the fuel economy can be substantially enhanced with only partial preview.**

***Index Terms*—Energy management, optimization control, plug-in hybrid electric vehicle, predictive control.**

I. Introduction

PLUG-IN HYBRID ELECTRIC VEHICLES (PHEVs) are now making the transition from prototype concept to mass production. Plug-in versions of the Toyota Prius for instance, are expected to go on sale in 2011–2012. Similar to conventional hybrid electric vehicles, PHEVs can take advantage of regenerative braking and a reduction in engine size to operate more efficiently. In addition, by partly utilizing the cheaper and typically cleaner electric grid energy, PHEVs achieve a much better overall fuel economy than conventional hybrid vehicles; their environmental footprint may also be much smaller. The efficiency of a PHEV also relies on its power management strategy, the algorithm which determines the split of the power request between the combustion engine and electric drive [19]. The focus of this brief is on developing a real-time implementable power management strategy that uses terrain, traffic, and trip distance preview and can enhance energy utilization of PHEVs.

Manuscript received June 16, 2010; revised December 02, 2010; accepted December 30, 2010. Manuscript received in final form February 10, 2011. Recommended by Associate Editor U. Christen. This work was supported by research grants from the National Science Foundation (CMMI-0928533), Intermap Technologies, and the U.S. Army Tank Automotive Research, Development, and Engineering Center (TARDEC).

The authors are with the Department of Mechanical Engineering, Clemson University, Clemson, SC 29634 USA (e-mail: chenz@g.clemson.edu; avahidi@clemson.edu).

Color versions of one or more of the figures in this brief are available online at http://ieeexplore.ieee.org.

Digital Object Identifier 10.1109/TCST.2011.2115242

Typical power management schemes in production HEVs use rules, pre-optimized maps, or instantaneous optimization to reduce the fuel use while sustaining the state-of-charge (SOC) of the battery [4], [10]. For this, they rely on instantaneous information about power demand, the vehicle's velocity, and the battery's SOC. This is formalized in a family of Equivalent Consumption Minimization Strategies (ECMS) first introduced by [13] where the power-split ratio is found by an instantaneous optimization algorithm [11], [16], [21]. An HEV maintains the battery's SOC in a narrow operating band during the whole trip. However, in a PHEV maximum energy efficiency is achieved if the batteries are depleted to their minimum allowable charge by the end of a trip.

Existing energy management strategies for conventional HEVs cannot be directly transferred to a PHEV. It is possible to run the PHEV in its all-electric mode until the battery is nearly depleted and then switch to a charge-sustaining mode and run the PHEV similar to an HEV [3], [18]. The result however may be far from optimal; it can be shown that the fuel-optimal solution is one that blends the use of the combustion engine and the electric motor throughout the trip in a way that the battery is nearly depleted at the charging destination [18]. This in turn requires knowledge of future trip conditions such as the trip length and future power demands. In [25] we found that knowledge of future road elevation profiles is beneficial in energy management of HEVs. In [24] we showed that advance knowledge of trip length can contribute to fuel saving in PHEVs. Missing in our previous work [24] and [25] was a real-time implementable algorithm for systematic integration of long-horizon preview information.

With complete knowledge of future driving conditions, it is possible to generate the optimal energy management policy by solving a dynamic program (DP) such as in [12]. However, this is computationally demanding and is not suitable for the practical cases which have only *partial* preview. The authors of [7] propose the use of a two-scale DP solution for a PHEV: A higher-level DP that plans the battery's SOC based on approximate information for the entire trip and a lower-level shorter horizon DP that has more accurate information and tracks segmentally the SOC trajectory found at the higher level. While interesting, constraining the solution to track a "loosely" optimized SOC trajectory is a shortcoming of the approach in [7]; i.e., it does not fully adapt its policy to instantaneous values of the battery's SOC and driver demand.

This study differs from previous work in that it classifies four different levels of access to the future information for power management of a PHEV: 1) full knowledge of distance, future velocity, and upcoming terrain profile; 2) full knowledge of distance, upcoming terrain and estimated velocity; 3) knowledge of distance to the next charging station and elevation changes (if available); 4) no future information. Except for the first level

TABLE I
PARAMETERS OF THE SIMULATED PHEV

maximum engine power	120kW	maximum motor power	45kW
battery capacity	21.5 Ah	open-circuit voltage	267 V
reducer ratio	2	final drive ratio	10.5

with full future information, the brief proposes *real-time* control strategies. The real-time power management is decomposed into an instantaneous optimization and a (global) parameter estimation: the power management decisions are calculated by a computationally efficient local ECMS optimization and based on instantaneous driver demand and the battery's SOC. It is the unknown parameter of the local ECMS that depends on future driving conditions. With the second level of preview, local optimization parameters are estimated by a backward DP or backward ECMS sweep over the estimated future velocity and exact future 3-D terrain information. With the third preview level, the parameter of local ECMS is adjusted based on the remaining distance to the next charging station and elevation changes if included. The proposed algorithms are in the class of nonlinear model predictive control methods introduced in [6] with the cost functions derived from Pontryagin's minimum principle.

Section II presents the vehicle configuration and its simulation model. Section III summarizes the DP and ECMS control strategies and also includes the description of a rule-based control strategy which is used as a comparison baseline. Section IV proposes different *real-time* control algorithms in which ECMS is adopted for instantaneous optimization with parameters adjusted by different methods depending on the level of preview. In Section V two sets of simulation case studies are presented which lead to conclusions in Section VI.

II. PHEV Powertrain Configuration and Model

A midsize 2000 kg passenger vehicle with a parallel hybrid electric configuration is selected for this study. Parameter values and detailed performance maps for various powertrain components are extracted from the database of Powertrain System Analysis Toolkit (PSAT) simulation software developed by Argonne National Laboratory [1]. A 120 kW gasoline internal combustion engine and a 45 kW AC motor are selected. They are directly connected to a torque coupler followed by a 5-speed automatic transmission. The auxiliary energy storage unit is a 21.5 Ah lithium-ion battery pack, reasonably sized for a PHEV. A 60% depth of discharge results in 20–30 km all-electric range depending on the cycle. The key vehicle parameters are summarized in Table I.

The PSAT-based full-order powertrain model contains the vehicle velocity, the clutch input speed, and the SOC of the battery as its dynamic states with many other lookup tables and logical switches. Maintaining this level of complexity for developing an optimal power management scheme is neither practical nor necessary. In fact, the state critical to the power management is the slowly varying SOC of the battery [19]. Therefore a reduced-order model is developed which contains the battery's SOC as its only dynamic state. While there exist a number of complex models for lithium-ion batteries that take into account the dynamics of polarization effects [1], the battery here is modeled with its open-circuit voltage in series with a constant internal resistance; this simplifies the model while maintaining the main dynamic effects. SOC dynamics are described by

$$\frac{d}{dt}\mathrm{SOC}(t) = -\frac{V_{\mathrm{oc}} - \sqrt{V_{\mathrm{oc}}^2 - 4P_{\mathrm{batt}}R}}{2\mathrm{RC}} \tag{1}$$

where V_{oc} is the open-circuit voltage of the battery, P_{batt} is the battery's electric power, R is the internal resistance of the battery and connecting wires, and C is the battery capacity. More details can be found in [17]. In the reduced-order model we continue to use the PSAT lookup tables to model the engine fuel rate and motor losses. The fuel rate $\dot{m}_f$ is mapped from the engine torque T_{eng} and engine speed ω_{eng}

$$\dot{m}_f = f(T_{\mathrm{eng}}, \omega_{\mathrm{eng}}). \tag{2}$$

Here we assume the engine is in its hot condition. Another lookup table is used to relate the motor mechanical power P_m and the motor speed ω_m to output electrical power of the battery P_{batt}, as implied by

$$P_{\mathrm{batt}} = g(P_m, \omega_m). \tag{3}$$

The gear shifting strategy which is a function of wheel torque demand and vehicle velocity is also adopted from PSAT and implemented as a lookup map.

III. Energy Management Strategy

A PHEV can be operated in two modes: charge-depleting (CD) and charge-sustaining (CS). When the battery SOC is near its minimum value the PHEV is operated in the charge-sustaining mode by blending operation of the engine and the electric motor. The battery's SOC is maintained near a set value similar in operation to a conventional HEV, therefore all the energy management strategies for HEVs are transferable to PHEVs in the CS mode.

When the battery SOC is high, the PHEV is operated in the charge-depleting mode: the battery's charge is depleted to its minimum allowed value with either all-electric operation or blended operation of the electric motor and combustion engine [2]. Because the electric grid energy normally costs less than gasoline fuel energy, the ideal scenario is to run the PHEV in its all-electric mode for short trips between two charging stations. For trips longer than the all-electric range, blended operation of the electric motor and the combustion engine throughout the trip is shown to be more fuel efficient than all-electric depleting followed by charge sustaining [18]. The decision whether to operate the PHEV in all-electric charge-depleting mode or blended charge-depleting mode can be optimized by using the knowledge of future driving conditions.

A. Rule-Based Control Strategy

When the future power demands are unknown, the vehicle is initially operated in all-electric charge-depleting mode. During this period the engine could be turned on if the power/torque request exceeds the capability of the battery or the electric motor. When the battery nears minimum allowable charge, the operation is switched to the charge-sustaining mode. Because of the

relative ease of tuning and implementation, rule-based power management strategies have been widely used in industry. Examples of different rule-based strategies can be found in academic research papers such as [10], [12], and [15]. The rule-based strategy for charge-sustaining power management in this study is adopted from PSAT simulation software with more details shown in [25].

B. Optimal Control: DP and ECMS

Similar to conventional hybrid vehicles, maximizing the fuel economy of a PHEV can be explicitly formulated as a minimization of the following cost function [10]:

$$J_{x_t}(\mathrm{SOC}(t)) = \int_t^{t_f} \dot{m}_f(t,u)dt + \phi(\mathrm{SOC}(t), \mathrm{SOC}_f) \quad (4)$$

where $J_{x_t}(\mathrm{SOC}(t))$ denotes the cost-to-go at time t from position x_t given the current SOC $\mathrm{SOC}(t)$ to the final position at time t_f; u is the power-split ratio between the engine and the battery and is the control input. The term $\phi(\bullet)$ penalizes deviation of the final SOC SOC_f away from $\mathrm{SOC}(t)$; in the following discussion, this term is removed and replaced by an equality constraint i.e., $\mathrm{SOC}_f = \mathrm{SOC}_d$, where SOC_d is the desired SOC at the final time. The optimal solution should also be subject to the powertrain model equations, the constraints for physical limitations of components, and pointwise-in-time constraints for SOC operation.

Analytical solutions to the above optimization problem do not exist in general, due to its many constraints and nonlinearities. We employ the two algorithms that have been widely used for numerical solutions of the optimal energy management problem.

1) Dynamic Programming: In the ideal scenario that the future velocity and exact future power demands are known, the optimal power-split ratio that minimizes the cost function (4) subject to model equations and all constraints can be numerically obtained by solving a deterministic dynamic programming problem [12] according to Bellman's optimality principle.

2) ECMS: In the ECMS the above optimization problem is simplified to a minimization of the *instantaneous* (rather than integral) equivalent fuel rate $\dot{m}_{f,\mathrm{equ}}$ defined as [15]

$$\dot{m}_{f,\mathrm{equ}}(t,u) = \dot{m}_f(t,u) + s(t) \cdot \frac{P_e(t,u)}{H_f} \quad (5)$$

where $P_e(t,u)$ is the net power charged to the battery or the power drawn from the battery including the power lost to the electric circuit's resistance; $s(t)$, normally abbreviated as s, is a fuel equivalence factor to convert electricity to equivalent fuel; and H_f is the lower heating value of the fuel.

With known future power demands, it is possible to find the true value for the equivalence factor $s(t)$. This can be better understood by using Pontryagin's minimum principle. The Hamiltonian for the cost function (4) is

$$H(\mathrm{SOC}(t), u, t) = \dot{m}_f(t,u) + \lambda(t)\dot{\mathrm{SOC}}(t) \quad (6)$$

where $\lambda(t)$ is the co-state and its optimal value depends on future power demands. Following Pontryagin's minimum principle, the co-state $\lambda(t)$ has the following dynamics [22]:

$$\dot{\lambda}(t) = -\frac{\partial H(\mathrm{SOC}(t), u, t)}{\partial \mathrm{SOC}(t)} = -\lambda(t)\frac{\partial \dot{\mathrm{SOC}}(t)}{\partial \mathrm{SOC}(t)} \quad (7)$$

subject to the equality constraint $\mathrm{SOC}_f = \mathrm{SOC}_d$. Using I to denote the battery's current, we substitute the dynamics of the SOC $\dot{\mathrm{SOC}}(t) = -I/C$ and $P_e(t,u) = IV_{\mathrm{oc}}$ into (6) and obtain

$$H(\mathrm{SOC}(t), u, t) = \dot{m}_f(t,u) - \frac{\lambda(t)H_f}{V_{\mathrm{oc}}C}\frac{P_e(t,u)}{H_f}. \quad (8)$$

Defining

$$s(t) = -\frac{\lambda(t)H_f}{V_{\mathrm{oc}}C} \quad (9)$$

yields the same equation as in (5). The challenge in finding the correct value of $s(t)$ for any given cycle can be seen by observing its dependence on the co-state $\lambda(t)$ in (9). The optimal value of the co-state $\lambda(t)$ should ensure $\mathrm{SOC}_f = \mathrm{SOC}_d$ and this strongly depends on the upcoming power demands. Therefore the optimal value of $s(t)$ is a function of future driving conditions as well as the current value of the battery's SOC. Due to uncertain future power demands, the true value of $s(t)$ can not be found, but we can come up with an estimate $\hat{s}(t)$ by utilizing partial preview information, as described in the next section.

IV. Estimation of Equivalence Factor With Partial Preview

A. Optimal Control With Partial Preview: Future Terrain, Trip Length, and Estimated Trip Velocity

The future power demand is a function of upcoming road slope and future velocity profile. The road terrain information can be retrieved accurately from in-vehicle 3-D maps and the vehicle GPS-based navigation system if the route is known *a priori*. As for the velocity, it is possible to estimate it using real-time traffic data streams or by using historical traffic data [8], [9]. The focus in this brief, however, is not on a method of velocity estimation; rather we focus on how such an estimate can be used in real-time energy management of PHEVs.

1) Estimating the Equivalence Factor Using DP: From the Hamilton-Jacobi-Bellman equation, we know that the partial derivative of the optimal cost with respect to the state is equal to the optimal co-state $\lambda^*(t)$ [22], that is

$$\lambda^*(\mathrm{SOC}(t), x_t) = \frac{\partial J^*_{x_t}(\mathrm{SOC}(t))}{\partial \mathrm{SOC}(t)} \quad (10)$$

where $\lambda^*(\mathrm{SOC}(t), x_t)$ is the optimal co-state as a function of $\mathrm{SOC}(t)$ and position x_t, and $J^*_{x_t}(\mathrm{SOC}(t))$ is the optimized cost-to-go in (4). Note that $\lambda^*(t)$ has been reformed as $\lambda^*(\mathrm{SOC}(t), x_t)$. Therefore, using (9) and (10) we have,

$$s^*(\mathrm{SOC}(t), x_t) = -\frac{\partial J^*_{x_t}(\mathrm{SOC}(t))}{\partial \mathrm{SOC}(t)}\frac{H_f}{CV_{\mathrm{oc}}}. \quad (11)$$

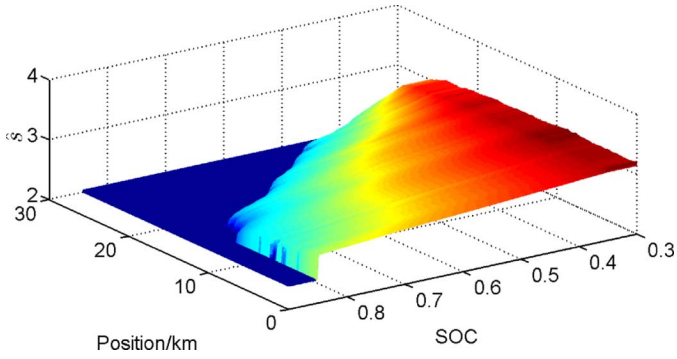

Fig. 1. Estimate $\hat{s}$ as a function of *SOC* and position in the 3-D plane.

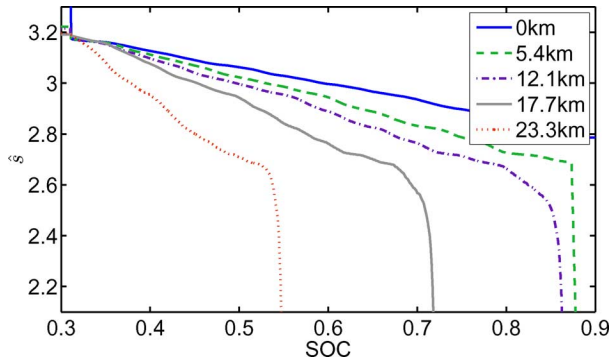

Fig. 2. Estimate $\hat{s}$ as a function of *SOC* and position in the 2-D plane.

With an estimate of future power demands, it is possible to execute a dynamic program backward in time which will calculate, for any possible pair $(\mathrm{SOC}(t), x_t)$, an estimate of the optimal cost-to-go denoted by $\hat{J}^*_{x_t}(\mathrm{SOC}(t))$. Finally, the estimate $\hat{s}$ is expressed as

$$\hat{s}(\mathrm{SOC}(t), x_t) = -\frac{\partial \hat{J}^*_{x_t}(\mathrm{SOC}(t))}{\partial \mathrm{SOC}(t)} \frac{H_f}{C V_{\mathrm{oc}}}. \tag{12}$$

Because DP calculates the cost-to-go backward in time, the $\hat{s}$ value obtained from the above formula will not depend on the past but only on future power demands. Thus a single round of DP computations may be enough for a trip as long as the estimated future power demand does not change significantly. Fig. 1 maps out values of $\hat{s}$ calculated using (12) for a simulation case which is used later in our discussion. In the figure, a low $\hat{s}$ value implies using electric power is cheaper than using fuel and therefore encourages the use of the battery. A high $\hat{s}$ value on the other hand discourages the use of the battery. As can be seen in Fig. 1, the value of $\hat{s}$ is mostly between 2 and 3.2 but drops at high SOC values or when the trip is nearly complete. In other words, the controller discharges the battery more aggressively when it anticipates that the charge left in the battery meets the energy needed to reach the destination. The value of $\hat{s}$ depicted in 2-D at different positions is shown in Fig. 2. It can be seen that the s-curve becomes steeper and more sensitive to the battery's SOC when the vehicle approaches its destination. We refer to this method of estimating the equivalence factor by using DP as D-ECMS in the following discussions.

2) Estimating the Equivalence Factor Using Backward ECMS: Real-time calculation of the equivalence factor using dynamic programming is viable but requires at least one backward sweep which, depending on the selected grid size and the processor, can be computationally demanding. In order to cut the computational load, here we propose the use of a backward ECMS, inspired by DP, for estimating the s value. It is possible to run the ECMS backward in time given the final SOC as SOC_d and to iterate on the value of s that yields the present SOC. More specifically we propose the following steps.

1) The range of the equivalence factor s is $[s_e, s_0]$ and is estimated as in [24], where s_e is the conversion ratio of fuel and electricity price explained in Section IV-B and s_0 is the neutral equivalence factor for a charge-sustaining HEV [25].
2) The range $[s_e, s_0]$ is discretized and the optimal SOC trajectory is obtained backward for each discretized s value in this range starting with the final SOC $\mathrm{SOC}_f = \mathrm{SOC}_d$. By changing time variable $\tau = t_f - t$ the SOC dynamics in (1) and co-state dynamics in (7) can be rewritten backwards-in-time

$$\frac{d}{d\tau}\mathrm{SOC} = \frac{V_{\mathrm{oc}} - \sqrt{V_{\mathrm{oc}}^2 - 4P_{\mathrm{batt}}R}}{2RC} \tag{13}$$

$$\frac{d}{d\tau}\lambda = -\lambda(\tau)\frac{\partial(\frac{d\mathrm{SOC}}{d\tau})}{\partial \mathrm{SOC}}. \tag{14}$$

However, this is a two-point boundary value problem and computationally expensive due to the coupling of the SOC and co-state dynamics in (13) and (14). To reduce the computation time for an online implementation, the co-state (and therefore the equivalence factor) are assumed to be constants in each backward run of ECMS. This is a valid assumption if: 1) the pointwise-in-time constraints on SOC are relaxed and 2) the righthand side of SOC dynamics in (1) is not an explicit function of SOC. The latter is true when the open-circuit voltage of the battery V_{oc}, and the battery resistance R, and capacity C, are constants. These assumptions yield $\dot{\lambda}(\tau) = 0$ and a constant optimal equivalence factor s. Considering the variation of the battery's parameters, a constant estimation of the equivalence factor does not result in a globally optimal solution. However, we note that the estimation error of the future driving conditions may have a larger impact on the equivalence factor than the variation in battery parameters and therefore the latter may not significantly influence the results. At each position x_t and based on the latest preview information the backward ECMS is executed starting with the final SOC equal to SOC_d; this is repeated for different initial guesses of the equivalence factor $s_i \in [s_e, s_0]$. Each run results in an optimal *SOC* trajectory as shown in Fig. 3.
3) The value of s that yields the present SOC of the battery is selected as the optimal value. Interpolations are performed when necessary. Note that this optimal value will be recalculated at each step in time based on the latest preview information.

The computation time for the above backward ECMS approach on a personal computer is much shorter than running the

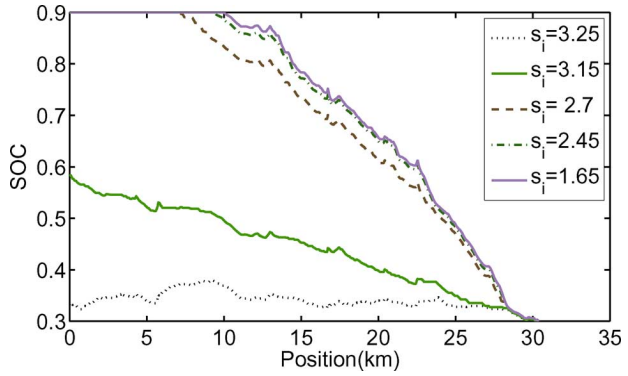

Fig. 3. Optimized SOC trajectories with the same terminal SOC (SOC_f) and different initial guesses (s_i) of the equivalence factor.

DP and thus it is thought to be very promising for a real-time implementation. Besides, because of its faster execution, the prediction of the future can be updated periodically which potentially enhances the performance of this methodology. We refer to this method of estimating the equivalence factor by a backward ECMS as E-ECMS.

B. Optimal Control With Partial Preview: Distance to the Next Charging Station and Hilly Road Terrain

A desired scenario is to estimate the equivalence factor without velocity information. In [5], [14], [20], and [25] different methods were proposed for estimating the equivalence factor in a charge-sustaining HEV. In the PHEV case, because the batteries can also be charged from the electric power grid, these approaches for estimating the equivalence factor s do not directly apply. A fair valuation of s can benefit greatly from: 1) information about the distance to the next charging station as compared to the all-electric range of the vehicle and 2) price of grid energy as compared to price of fuel energy. Remember s, by the definition, is the conversion ratio between electricity and fuel. Therefore the first step is to find the price ratio r between electricity and fuel defined by

$$r = \frac{\frac{Pr_f s_0 C_s}{(\rho H_f)}}{\frac{Pr_e}{\bar{\eta}_e}} \tag{15}$$

where Pr_f is the fuel price; ρ is the density of the fuel; C_s is the constant conversion ratio between different units; Pr_e is the electricity price; $\bar{\eta}_e$ is the charging efficiency from charging stations to a PHEV. s_0 is the estimated conversion ratio from electricity to fuel for a charge-sustaining HEV [25] based on the average efficiency of the powertrain.

When the traveling distance is known to be less than or equal to the vehicle's electric range, the powertrain can be run in its all-electric mode. The equivalence factor s_e for this mode is then calculated as

$$s_e = \frac{s_0}{r}. \tag{16}$$

Combining (15) and (16) yields

$$s_e = \frac{\frac{Pr_e}{\bar{\eta}_e}}{\frac{Pr_f C_s}{(\rho H_f)}}. \tag{17}$$

Note that in the above equation, s_e is not a function of the neutral equivalence factor s_0. On the other hand, when the traveling distance is known to exceed the all-electric range, the equivalence factor should be adjusted up to reflect the use of gasoline fuel energy during the trip. We define a ratio parameter κ as follows to relate the nominal all-electric range X_e and the total trip distance X

$$\kappa = \min\left(\frac{X_e}{X}, 1\right) \tag{18}$$

and determine an averagely estimated equivalence factor $\hat{s}$ as an initial guess

$$\hat{s} = s_e + \sqrt{1-\kappa^2}(s_0 - s_e). \tag{19}$$

In the above equation when $X_e \geq X$ then the equality $\hat{s} = s_e$ reflects the fact that all of the electricity will be provided by the grid. At the other extreme, when the electric range X_e is much smaller than the distance to the next charging station X such that $\kappa \approx 0$, then $\hat{s} = s_0$ which reflects the average electric price in the charge-sustaining mode. In between, when $0 < \kappa < 1$, a value of $\hat{s}$ between s_0 and s_e is chosen as the base equivalence factor.

To reflect the influence of the current SOC in the selection of the equivalence factor, one can redefine the parameters κ and $\hat{s}$ as follows:

$$\kappa(t) = \min\left(\frac{x_e(t)}{x_r(t)}, 1\right) \tag{20}$$

$$\hat{s}(\mathrm{SOC}(t), t) = s_e + \sqrt{1-\kappa(t)^2}(s_0 - s_e) \tag{21}$$

where $x_e(t)$ is the all-electric range for the remaining SOC and $x_r(t)$ is the remaining trip distance. They are defined as

$$\begin{aligned} x_e(t) &= \frac{\mathrm{SOC}(t) - \mathrm{SOC}_{\min}}{\mathrm{SOC}_{\max} - \mathrm{SOC}_{\min}} X_e \\ x_r(t) &= X - x_t \end{aligned} \tag{22}$$

where $\mathrm{SOC}_{\max}$ and $\mathrm{SOC}_{\min}$ are the upper and lower operation bounds of the battery's SOC. By its definition, the equivalence factor $\hat{s}$ varies between s_e and s_0 depending on the current SOC $\mathrm{SOC}(t)$ and remaining trip distance. The dependence of the s value on four parameters s_0, s_e, $\mathrm{SOC}(t)$, and remaining trip distance $x_r(t)$ reduces its sensitivity to the estimation of s_0; this is unlike a charge-sustaining HEV. The ECMS discussed in this part is referred as B-ECMS since it blends operation of the engine and the electric motor and discharges the battery gradually. This is similar to the methods proposed in [23], [24] but without the assumption of tracking a predefined SOC trajectory.

In a hilly terrain where more gravitational potential energy is available in descents to drive the vehicle, the assumption of discharging the battery gradually may not be a good one. Observing this fact, here we propose an adjustment to the B-ECMS strategy to account for the influence of large elevation changes. The availability of gravitational potential energy in descents can be translated into an extension of the all-electric range. The adjusted all-electric range $x'_e(t)$ including the extension is defined as

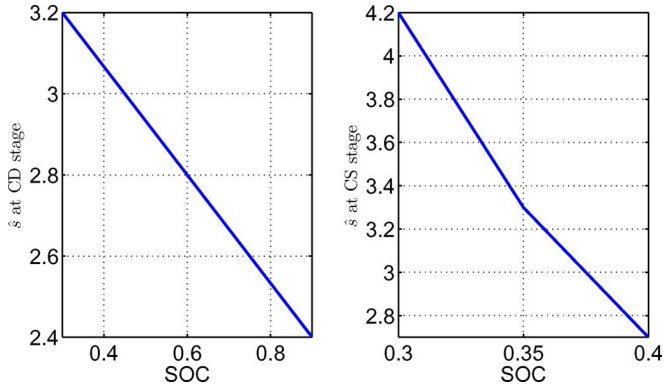

Fig. 4. Estimate $\hat{s}$ as a function of *SOC* at different stages: charge-depleting (CD) stage and charge-sustaining (CS) stage.

TABLE II
COST GAP (%) OF DIFFERENT CONTROL STRATEGIES COMPARED WITH DP WITH TRIP DISTANCE OF 32, 48, 72 km IN CASE STUDY I

Gap(%)		32km	48km	72km
preview	D-ECMS	0.73	0.66	0.39
	E-ECMS	0.76	0.69	1.18
	B-ECMS	1.62	0.65	0.91
no preview	DS-ECMS	2.90	2.67	3.59
	Rule-based	8.88	7.88	8.61

$$x'_e(t) = x_e(t) + \frac{\frac{mg\Delta h\bar{\eta}_r}{(\bar{V}_{\rm oc}C)}}{\mathrm{SOC}_{\max} - \mathrm{SOC}_{\min}} X_e \qquad (23)$$

where m is the vehicle's mass; g is the gravitational acceleration; $\bar{V}_{\rm oc}$ is the average battery voltage; $\bar{\eta}_r$ is the average recuperation efficiency; we set $\bar{\eta}_r = 1$ when the potential energy is not lost to braking. Δh is the downhill elevation change and defined as: $\Delta h = \max\left(H(\tau > t)\right) - H(t_f)$, where $H(\bullet)$ is the elevation at time $(\bullet)$, t denotes the current time, and τ is the future trip time. Note that Δh is a non-negative value. We use $x'_e(t)$ to replace the term $x_e(t)$ in (20).

C. Optimal Control Without Preview

In the absence of preview, one can guess a low value for the equivalence factor initially and increase it when the SOC decreases. This ensures that the battery is discharged aggressively at high SOC and conservatively at low SOC. When the SOC reaches its lower bound (here 0.3), the control strategy is switched to a charge-sustaining strategy which keeps the SOC in a narrow operating band e.g., between 0.3 and 0.4. In this brief, we refer to this strategy as depleting and sustaining ECMS (DS-ECMS). This is shown in Fig. 4 where the equivalence factor s is chosen to be a linear function of SOC in the charge-depleting (CD) stage and a piece-wise linear function in the charge-sustaining (CS) stage with details shown in [25]. A summary of different control strategies as well as their abbreviations is shown in Table IV at the end of this brief.

V. SIMULATION ANALYSIS

The performance of the proposed methods is studied via two sets of simulations. The first is a federal test cycle and a real-world terrain profile. The second uses velocity and terrain data

TABLE III
COST GAP (%) OF DIFFERENT CONTROL STRATEGIES COMPARED WITH DP IN CASE STUDY II (R1-ROUTE 1, R2-ROUTE 2, R3-ROUTE 3 IN FIG. 6, R4-FLAT ROAD WITH VELOCITY FROM R2)

Gap(%)		R1 uphill & downhill	R2 uphill	R3 downhill	R4 flat
preview	E-ECMS	2.74	1.03	6.46	6.33
	B-ECMS	8.53	2.81	39.56	2.77
	B-ECMS (adjusted)	0.75	-	5.00	-
no preview	DS-ECMS	7.28	4.82	16.55	8.34
	Rule-based	14.20	14.81	20.77	15.70

TABLE IV
COMPUTATIONAL CASE STUDY FOR PROPOSED CONTROL STRATEGIES

Algorithm	Method to estimate equivalence factor s	CPU time
D-ECMS	by DP	600s
E-ECMS	by ECMS	2.5s
B-ECMS	by blending operation	0.7s
DS-ECMS	by depleting and sustaining operation	0.7s

obtained simultaneously from driving in a mountainous area. The total energy cost, taking into account both fuel and electricity consumption, is used as the index for evaluating the performance of different strategies. The price of gasoline and electricity, which may vary by area and time, are set to \$0.79/litre (\$3/gallon) and \$0.12/kWh, respectively.

A. Case Study I

The terrain and velocity profile for this simulation case study are shown in Fig. 5. The terrain is a stretch of uphill road in Contra Costa County in California and is extracted from Intermap Technologies' 3-D map database and the velocity profile is that of the EPA Highway Fuel Economy Cycle (HWFET). Because the fuel economy of a PHEV strongly depends on the trip distance, three simulation distances of 32, 48, and 72 km are selected which are respectively 1.6, 2.4, and 3.6 times the all-electric range. The velocity profiles are repeated for long distance simulations; the grades are mirrored, and then also repeated if necessary. A simple method to estimate the velocity is deployed in which the vehicle is forced to run with the speed limits along the road. In the simulation the speed limits, observed from the HWFET cycle data, are set at 20 and 25 m/s for the two different segments. The acceleration/deceleration of the vehicle is set to the constant value 0.5 m/s^2. The real and estimated velocity profiles are shown in Fig. 5. In practice it is deemed feasible to estimate a vehicle's future speed by using known speed limits, traffic signal location and timing information, and real-time traffic flow conditions [7].

In each simulation case study, dynamic programming with full future information can find the lowest energy cost; we use this lowest cost as the best benchmark. The performance of other proposed methods is evaluated by calculating their percent energy cost difference with respect to the DP benchmark. Table II summarizes these results. When preview is available the cost gap of different control strategies compared with DP is generally less than 1%. We are also interested in determining which parts of future information are important for reducing the energy cost. It can be seen that B-ECMS with only trip distance information performs very close to D-ECMS and E-ECMS and is not far from the best possible benchmark, implying that knowledge

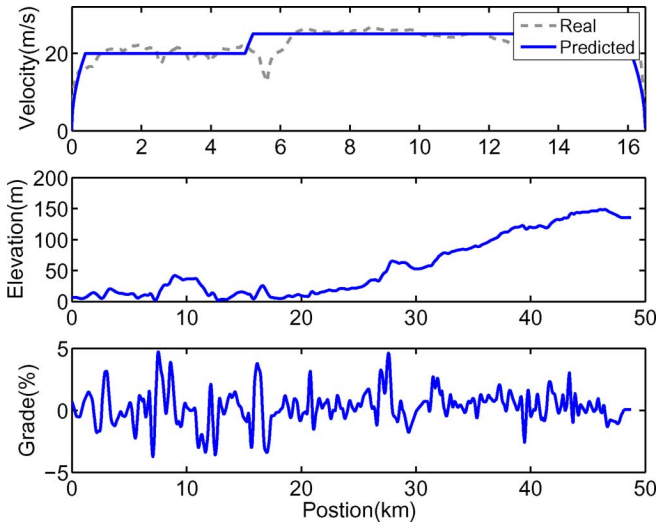

Fig. 5. Velocity, elevation, and grade profiles for Case Study I.

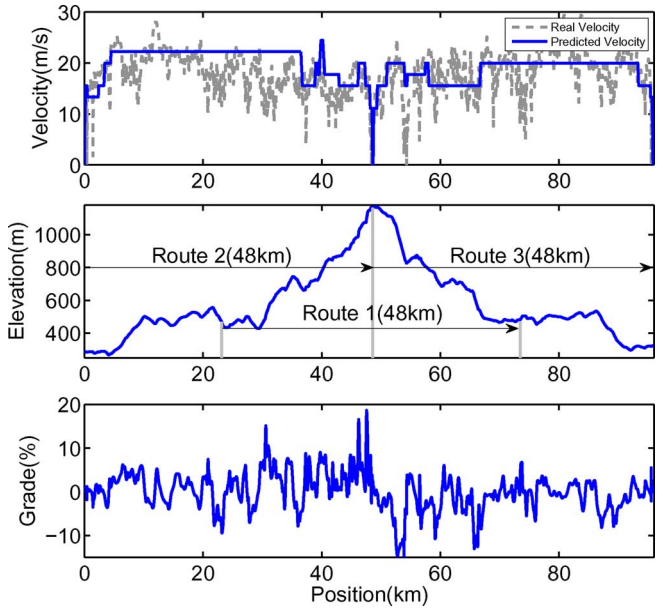

Fig. 6. Velocity, elevation, and grade profiles for Case Study II.

of trip distance is a significant factor for energy cost saving for a PHEV and that the influence of non-hilly terrains to an estimation of the equivalence factor can be ignored. Without preview, the energy cost would increase considerably as shown in the results of DS-ECMS and rule-based strategies.

B. Case Study II

To evaluate the influence of larger changes in elevation, we drove a vehicle starting from the city of Clemson in South Carolina to the town of Highlands in North Carolina and back, mostly via the hilly US-28 road on May 14th, 2010. The elevation change in this trip was more than 900 m over a distance of almost 50 km. We recorded both the velocity and elevation using a Garmin GPS 20 $\times$ receiver with a sampling time of 1 s. The raw data from the GPS was refined by removing the dead points and by interpolating the missed data. For the simulation case study, we divide the trip into three segments all having the same trip length (48 km) with a combination of uphill and downhill profiles (*Route 1*), an uphill profile (*Route 2*), and a downhill profile (*Route 3*) as shown in Fig. 6. The predicted speed in this figure reflects the speed limits observed from the road side signs which we had recorded separately as a function of trip time. To isolate the influence of velocity, we also designated a fourth scenario denoted by *Route 4* with the same velocity profile of *Route 2* but with road grade set to zero. *Route 1*, *Route 2*, *Route 3*, and *Route 4* are abbreviated as *R1*, *R2*, *R3*, and *R4*, respectively, in the following discussion.

Similar to the Case Study I, DP with full future information is used as the best benchmark. Table III summarizes the energy cost gap between strategies with and without preview and the DP benchmark. Here D-ECMS results are not reported as they are similar to those of E-ECMS. As shown in the table, E-ECMS performs closest to DP for the *R2* uphill terrain with the cost gap of only 1%. The difference is larger for the *R3* downhill terrain (6.46%) and for the flat case of *R4* (6.33%). Note that on steep uphill roads the power demand from the grade dominates that of demand to changes in velocity; thus poor estimation of velocity may have less influence on the optimality of E-ECMS solution. On downhill or flat terrain on the other hand the power demand caused by changes in velocity dominates and therefore the uncertainty about the future velocity profile results in a larger cost gap between E-ECMS and DP.

As seen in this table, the trip distance based B-ECMS strategy is far from optimal especially when there are large downhill elevation changes (e.g., 40% worse than DP for *R3*). During descents there are frequent opportunities for running electric only or for regeneration; but because B-ECMS estimates the equivalent fuel factor based on the remaining trip distance only, it fails to capture part of the available potential energy. This demonstrates the importance of incorporating potential energy in the estimation of an equivalence factor in occasions where large elevation changes exist. The performance of adjusted B-ECMS for (partial) descent routes *R1* and *R3* is shown in Table III and is much improved. Note that E-ECMS sometimes performs worse than (adjusted) B-ECMS. This may be attributed to large velocity transients in this case study which cannot be merely captured by using the speed limit approximation as done in E-ECMS. We observe that the algorithms with partial preview always perform better than strategies without preview.

C. Computational Case Study

Besides the energy cost, we also compared the computational burden in a simulation with total trip time of 1472 s and sampling time of 2 s. The SOC resolution was set at 0.0001 for all simulations. The simulations were performed on a personal computer with a CPU speed of 1.8 GHz and memory of 2 GB. Table IV summarizes the computational time of each algorithm. It can be seen that the E-ECMS approach runs much faster than D-ECMS with the same level of preview without much loss in performance and has the potential to be used in real-time. The computational burden of B-ECMS and DS-ECMS is essentially the same as a normal ECMS approach and thus it is suitable for real-time optimization.

VI. Conclusion

This brief investigated real-time implementable energy management algorithms for energy management of plug-in hybrid vehicles that can take advantage of information preview for fuel saving. This is achieved by handling the energy minimization problem at two levels: 1) a global optimization approach that utilizes preview information (if available) for the whole trip to estimate a fuel-electricity equivalence parameter and 2) a local ECMS optimization which determines the optimal control based on instantaneous values of power demand, the battery's SOC, and the parameter set by the global optimizer. A simulation case study with a federal driving cycle (HWFET) indicated that knowledge of distance to the next charging station can have a significant influence on the fuel economy of a PHEV because it allows better planning of all-electric or blended motor/engine operation. Full terrain preview and estimated future velocity preview can result in additional fuel economy improvements of up to 1%. Another simulation case study with large elevation changes indicated the importance of accounting for potential energy gains resulting from elevation changes. Predicting the future velocity profile based on speed limits helps the energy management of a PHEV in general. If the real driving cycle has more velocity transients than the predicted one, the control strategy that relies only on trip length and elevation change and not on velocity estimate may perform better. The computational time required to include preview is shown to be much smaller than the total simulation time and therefore has the potential for a real-time implementation. This work focused only on the energy minimization. Future work can consider other factors such as total emissions of the vehicle and of the electric grid.

Acknowledgment

The authors would like to thank G. Mahler for his help in collecting the experimental data of the Case Study II, and for proofreading this manuscript.

References

[1] Argonne National Laboratory, Chicago, IL, "Powertrain System Analysis Toolkit-PSAT," 2010. [Online]. Available: http://www.transportation.anl.gov/software/PSAT/PSAT_Demo/index.html

[2] J. Axsen and K. Kurani, "The Early U.S. market for PHEVs: Anticipating consumer awareness, recharge potential, design priorities and energy impacts," 2008. [Online]. Available: http://pubs.its.ucdavis.edu/publication_detail.php?id=1191

[3] A. Burke and E. V. Gelder, "Plug-in hybrid-electric vehicle powertrain design and control strategy options and simulation results with lithium-ion batteries," 2008. [Online]. Available: http://phev.ucdavis.edu/publications/vehicle-architecture-and-control-systems

[4] K. L. Butler, M. Ehsani, and P. Kamath, "A Matlab-based modeling and simulation package for electric and hybrid electric vehicle design," *IEEE Trans. Veh. Technol.*, vol. 48, no. 6, pp. 1770–1778, Nov. 1999.

[5] A. Chasse, G. Hafidi, P. Pognant-Gros, and A. Sciarretta, "Supervisory control of hybrid powertrains: An experimental benchmark of offline optimization and online energy management," in *Proc. IFAC Workshop Engine Powertrain Control, Simulation Model.*, 2009, pp. 110–117.

[6] R. Findeisen and F. Allgöwer, "An introduction to nonlinear model predictive control," in *Proc. 21st Benelux Meet. Syst. Control*, 2002, pp. 1–23.

[7] Q. Gong, Y. Li, and Z. Peng, "Trip-based optimal power management of plug-in hybrid electric vehicles," *IEEE Trans. Veh. Technol.*, vol. 57, no. 6, pp. 3393–3401, Nov. 2008.

[8] Q. Gong, Y. Li, and Z. Peng, "Trip based optimal power management of plug-in hybrid electric vehicles using gas-kinetic traffic flow model," in *Proc. Amer. Control Conf.*, 2008, pp. 3225–3230.

[9] Q. Gong, Y. Li, and Z. Peng, "Power management of plug-in hybrid electric vehicles using neural network based trip modeling," in *Proc. Amer. Control Conf.*, 2009, pp. 4601–4606.

[10] L. Guzzella and A. Sciarretta, *Vehicle Propusion Systems: Introduction to Modeling and Opitmization*. New York: Springer, 2005, pp. 190–203.

[11] A. Kleimaier and D. Schröder, "An approach for the online optimized control of a hybrid powertrain," in *Proc. 7th Int. Workshop Adv. Motion Control*, 2002, pp. 215–220.

[12] C.-C. Lin, H. Peng, J. W. Grizzle, and J.-M. Kang, "Power management strategy for a parallel hybrid electric vehicle," *IEEE Trans. Control Syst. Technol.*, vol. 11, no. 6, pp. 839–849, Nov. 2003.

[13] G. Paganelli, S. Delprat, T. Guerra, J. Rimaux, and J. Santin, "Equivalent consumption minimization strategy for parallel hybrid powertrains," in *Proc. Veh. Technol. Conf.*, 2002, vol. 4, pp. 2076–2081.

[14] G. Paganelli, Y. Guezennec, and G. Rizzoni, "Optimizing control strategy for hybrid fuel cell vehicle," *SAE Special Pub. 1691, Fuel Cell Power for Transport.*, 2002. [Online]. Available: http://papers.sae.org/2002-01-0102/

[15] P. Pisu and G. Rizzoni, "A comparative study of supervisory control strategies for hybrid electric vehicle," *IEEE Trans. Control Syst. Technol.*, vol. 15, no. 3, pp. 506–518, May 2007.

[16] G. Rizzoni, P. Pisu, and E. Calo, "Control strategies for parallel hybrid electric vehicles," in *Proc. IFAC Symp. Adv. Autom. Control*, 2004, pp. 508–513.

[17] D. Rotenberg, A. Vahidi, and I. Kolmanovsky, "Ultracapacitor assisted powertrains: Modeling, control, sizing, and the impact on fuel economy," *IEEE Trans. Control Syst. Technol.*, to be published.

[18] A. Rousseau, "PHEV vehicle level control strategy summary," 2008. [Online]. Available: http://www.transportation.anl.gov/pdfs/HV/552.pdf

[19] A. Sciarretta and L. Guzzella, "Control of hybrid electric vehicles," *IEEE Control Syst. Mag.*, vol. 27, no. 2, pp. 60–70, Apr. 2007.

[20] A. Sciarretta, L. Guzzella, and M. Back, "A real-time optimal control strategy for parallel hybrid vehicles with on-board estimation of control parameters," in *Proc. IFAC Symp. Adv. Autom. Control*, 2004, pp. 502–507.

[21] A. Sciarretta, M. Back, and L. Guzzella, "Optimal control of parallel hybrid electric vehicles," *IEEE Trans. Control Syst. Technol.*, vol. 12, no. 3, pp. 352–363, May 2004.

[22] R. F. Stengel, *Optimal Control and Estimation*. New York: Dover, 1994, pp. 204–207.

[23] P. Tulpule, S. Stockar, V. Marano, and G. Rizzoni, "Optimality assessment of equivalent consumption minimization strategy for PHEV application," in *Proc. ASME Dyn. Syst. Control Conf.*, 2009, pp. 265–272.

[24] C. Zhang, A. Vahidi, X. Li, and D. Essenmacher, "Role of trip information preview in fuel economy of plug-in hybrid vehicles," in *Proc. ASME Dyn. Syst. Control Conf.*, 2009, pp. 253–258.

[25] C. Zhang, A. Vahidi, P. Pisu, X. Li, and K. Tennant, "Role of terrain preview in energy management of hybrid electric vehicles," *IEEE Trans. Veh. Technol.*, vol. 59, no. 3, pp. 1139–1147, Mar. 2010.